Available online at www.sciencedirect.com

SciVerse ScienceDirect

Procedia Engineering 58 (2013) 550 – 559

Procedia Engineering

www.elsevier.com/locate/procedia

The 12th Hypervelocity Impact Symposium

# A Novel Technique for High-Velocity Launch of an Impactor for Initiating Shock-to-Detonation in High Explosives

Sean K. Treadway[a]*, Andrew N. Lloyd[a]

[a]*Corvid Technologies, 145 Overhill Dr, Mooresville, NC, 28117*

**Abstract**

This paper is relevant to the matter of high-velocity launch of a projectile by a small scale system that might be used to initiate high explosive (HE) or in shock phenomenology work. A small-scale launcher was designed to initiate detonation in HE, function selectively based on inputs, and be easily integrated into a larger system. Under these design constraints the launcher mass and volume had to be minimized while retaining robust function. The basic goal of the launcher was to drive a flyer to critical velocities that will produce shock-to-detonation (SDT) in high explosive upon impact. The flyer was propelled by explosive compression of a polystyrene buffer to pressures greater than 20 GPa. The entire launcher assembly was less than 8 cm in length and 1.5 cm in diameter. A 0.6 cm flyer was launched at 2.4 km/s and maintained flight stability. Launcher design and the SDT response due to flyer impact were modelled using CTH computer simulations. Testing with launchers in both stand-alone and integrated configurations showed reliable, expected function. Both simulation and test results are presented.



Selection and peer-review under responsibility of the Hypervelocity Impact Society

*Keywords*: Launch, Shock-to-detonation, High Velocity, Shock

## 1. Introduction

Modern explosive formulations have been engineered to be highly insensitive to shock loading that might lead to detonation. Initiation of these formulations typically requires a firing train (MIL-STD-1316E, 1998 [1]) that includes an electrically driven detonator and a relatively sensitive booster charge that is placed in direct contact with the main charge. The firing train is not installed until munitions are ready for use.

Novel munition designs may require that main charges having initiation points on the interior, and these locations might be impractical to access for firing train installation. To address this problem we have devised a method for interior detonation that does not involve a typical firing train and can be embedded in a munition during manufacture. This method involves the launch of a flyer disk at high velocities to produce main charge initiation from shock-to-detonation (SDT) at specific locations inside a munition. This paper describes the development of the embedded flyer launch mechanism. The launcher consists of a high explosive (HE) driver, inert buffer, and flyer disk. Initiation of the HE driver compresses the buffer, which in turn transmits a propulsive shock to the flyer disk. The flyer disk is intended to produce SDT in a target HE.

It was necessary to create a compact and light weight launcher in order to minimize quantity of munition main charge displaced and to minimize parasitic mass. Loss of main charge and unnecessary added mass can adversely affect various

* Corresponding author. Tel.: 704-799-6944.
*E-mail address:* sean.k.treadway@corvidtec.com.


Selection and peer-review under responsibility of the Hypervelocity Impact Society
doi:10.1016/j.proeng.2013.05.063

aspects of munition performance. Similar launcher schemes, such as the fast shock tube (FST) studied by Meier [2] and Marsh [2], have been used in laboratory settings for equation-of-state research. That approach also used an explosively compressed coaxial buffer, and was capable of accelerating flyers to velocities in the range of 6 to 9 km/s over a few cm. The FST and it variants were larger in scale than our launcher, being tens of cm long and launching flyers up to 2.54 cm in diameter. Flyer propulsion in the FST resulted from compressed buffer material acting to create high pressures on the back of the flyer. In contrast, our flyer is driven by momentum transfer from shock transmitted from the buffer to the flyer, which accelerates the flyer to maximum velocity within 3 μs and having travelled less than 0.3 cm. This high acceleration is necessary because of the volume constraints on the launcher assembly. Another distinction is that our design had to be robust enough function outside of a controlled lab environment.

In this paper we describe the development of the launcher in the context SDT initiation of a HE main charge. Our primary goal is to describe the design of the launcher. Requirements for SDT drive flyer design, so extensive discussion of shock impact initiation is included. However, the SDT response of a given HE is secondary in our presentation.

We lay out how the launcher functions, and how the required flyer size, material, and velocity for target SDT were determined. The flyer parameters were initially explored using 1-dimensional shock calculations. After this scoping effort, high-fidelity 3-dimensional (3-D) hydrocode calculations were conducted that examined launcher function and target HE SDT response using reactive burn models. We show that the concept was matured and evaluated using computer simulations to explore the design space, making extensive refinements and simplifications prior to building physical prototypes. Tests were conducted of the resulting design, and the results will be discussed in brief.

## 2. Launcher concept

The initial concept grew out of a larger development effort and failed approaches for initiating a specific point on a main charge interior without the use of a traditional firing train. These failures drove us toward the launcher concept in a somewhat organic fashion. What emerged was an early configuration that is shown in Fig. 1.

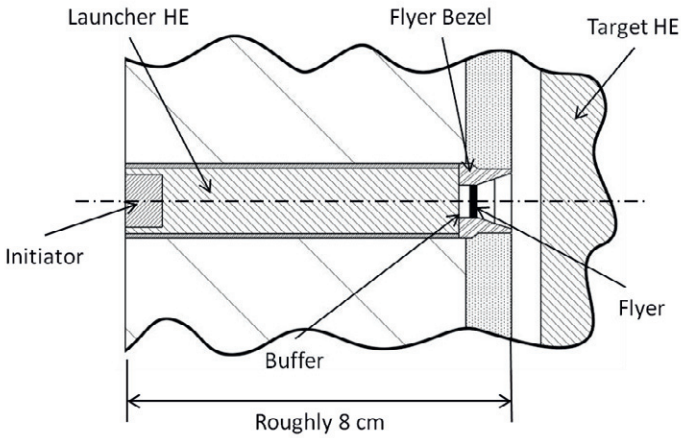


Fig. 1. Early launcher design integrated into notional munition.

The overall design objective was to project a flyer capable of causing an SDT response in a target HE. The launcher functions when an initiator detonates the launcher HE, creating a fairly planar detonation that creates a shock front in the buffer. This shock front propels the flyer into the target HE. The polymer buffer prevents the detonation wave from acting directly on the flyer, mitigating breakup. The steel bezel retains the flyer and limits reaction product flow around the flyer. Any sympathetic SDT response in the launcher HE from laterally impinging shockwaves results in a detonation wave that acts obliquely on the buffer and produces insufficient flyer velocity for target HE SDT. An additional objective was to keep cost of fabrication to a minimum by avoiding high precision machining and exotic materials.

## 3. Design Scoping

The HE used in the launcher needed to be something in common use. This minimizes trouble with sympathetic detonation sensitive criteria in the long run, and minimizes cost. PBXN-110 (previously designated PBXW-113) was identified as the SDT target of the launcher. N-110 was also initially used as the launcher explosive driver. N-110 is 88%

HMX and 12% binder, and is considered relatively insensitive (G. T. Sutherland, [4]).

Creating the smallest possible flyer was a key challenge. Flyer diameter must be minimized so that launcher volume is minimized. An understanding of target HE initiation and SDT response was critical because of the relationship to flyer size.

Result for wedge tests of N-110 are known to differ, but run distances of 0.3 cm exist in the data. Among the data sets the maximum threshold pressure for 0.3 cm run distance is approximately 13 GPa (OConnor, [5]). This 0.3 cm distance will serve as a benchmark for both the required diameter and thickness for the flyer.

Regarding flyer diameter, the nature of lateral relief waves in shocks created by planer impacting flyers dictates that the flyer diameter should be at least twice the run distance (Cooper, [6]). Also, N-110 has an experimentally determined failure diameter of roughly 0.6 cm for [4]. Based on these characteristics we believed a flyer near 0.6 cm might be feasible.

Jacob's-Roslund correlations for bare N-110 impacted by a steel projectile imply that a 0.6 cm projectile diameter would require an impact velocity of ~2.2 km/s (Hull, 2002[7]). This criterion was an extrapolation due to a lack of data points for diameters this small. However, it did indicate that SDT with a flyer this size might be realistic since we believed that flyer velocities above 2.2 km/s were possible.

To produce a sustained detonation the flyer thickness must be such that initial impact shock pressure is maintained through a minimum run distance. Based on wedge test data for N-110, this would be a square pulse of at least 13 GPa through 0.3 cm, and would qualify as a "thick-pulse." Detonation may also occur due to a "thin-pulse," with a square wave sustained through a distance of less than 0.3 cm. Persistence of shock pressures is determined by flyer thickness, as well as impact velocity, and flyer and target material shock response. The initial shock pressure decays as the relief wave propagates from the back of the flyer, through its thickness, and then catches the initial shock wave front in the target. The back of a flyer projected by the launcher is essentially a free surface.

## 4. Hydrocode Analysis

1-dimensional shock and Hugoniot relations were used to make estimates of flyer dimensions and impact velocities. The shock-particle velocity relations used for the N-110 came from combined light gas gun work and wedge test data [2], and N-110 density in this work was 1.68 g/cc. Assuming a steel flyer 0.15 cm thick impacting N-110 at 2.2 km/s, the shock pressure is calculated to be 14 GPa. This pressure would exist as a square pulse for 0.17 cm, prior to the arrival of the rarefaction wave from the back of the flyer. This .17 cm depth is less than the desired 0.3 cm distance, and can does not meet "thick-pulse" criteria for HE initiation. The 14 GPa pressure will travel a total depth of 0.57 cm before the rarefaction arrives at the leading edge. This pressure and distance might still produce SDT as a "thin-pulse". A thickness of 0.15 cm was indicated to be on the edge of what was possible for a small flyer. A minimum flyer thickness of 0.25 cm was calculated as necessary for creating a 14 GPa square pulse that would propagate 0.3 cm in to the HE. Hydrocode Modeling

Our approach used extensive hydrocode modeling to design a system for selective detonation of discrete HE sections. Prototypes were then constructed and tested. This approach short-circuits the traditional design-test cycle by reducing or eliminating design revisions that must be re-tested. Modern hydrocodes and Corvid's 6,000+ CPU massive parallel processing (MPP) computing resource allows conception, refinement, and evaluation of shock and detonation dominated systems prior to testing. The understanding gained from this approach enables intelligent instrumentation and data gathering from subsequent testing. The benefits are savings of time and money, and increased value from tests that are conducted.

The Eulerian hydrocode CTH (Sandia Corporation, 2012[8]) was the primary modeling tool in this effort. CTH has the capability to model all relevant phenomena and simulate the entire system on the appropriate time scale of hundreds of microseconds. Over 120 3-D calculations of this type were conducted.

Examination of work on development of burn model parameters for N-110 indicated some variation, as was the case with the wedge test data. However, O'Conner and Sewell conducted a fairly thorough examination of N-110 parameter validity for the History Variable Reactive Burn (HGRB) and Ignition and Growth (IGRB) models. Both models are implemented in CTH. They examined two sets of IGRB parameters. Their comparisons of code calculations to experimental failure diameter results and the Jacob's-Rosland formulation for fragment impact indicated that use of the IGRB model with the parameters listed in Table 1 would be the most accurate for small flyer analysis. These parameters were developed and refined by Miller and Sutherland [9]. The JWL model was used for both the reacted and unreacted N-110 equation of state (EOS).

Initial hydrocode calculations gauged SDT response using a conservative sized 1 cm flyer, of thicknesses of 0.12 cm and 0.25 cm, and impact velocities below 2.2 km/s. Flyers were simply given an initial velocity and not projected by the launcher. These simulations were carried out using a computational domain cell size of 0.020 cm.

Table 1: IGRB CTH parameters used for PBXN-110 SDT calculations [5]. Parameters not listed were set to 0.0.

| $G_0$ (dyne/cm$^2$)/sec | $s_0$ | a | $y_0$ | $w_0$ | $G_1$ (dyne/cm$^2$)/sec | $s_1$ | $q_1$ | $y_1$ | $w_1$ |
|---|---|---|---|---|---|---|---|---|---|
| 5 x $10^7$ | 0.667 | 0.001 | 4.0 | 0.15 | 1.15 x $10^{-27\text{-}12y_1}$ | 0.667 | 0.222 | 3.0 | 1.0 |

James [10] and Walker et al. [11] have shown a correlation between detonation initiation and impact shock critical energy, $E_c$, deposited into HE by an impactor. Calculation of impact shock energy deposited in the HE allowed comparison of flyer configurations and impact velocities that lead to SDT in the models. Also it allowed a threshold, $E_c$, to be established for the purpose of launcher design. The impact shock energy, E, in the HE can be calculated as,

$$E = \frac{P^2 \tau}{\rho_0 U}$$

where $P$ is peak shock pressure in HE, $\tau$ is duration of peak pressure pulse before the rarefaction wave arrives from rear of impactor, $\rho_0$ is initial HE density, and $U$ is shock velocity in HE [11]. If $E$ exceeds $E_c$ then detonation is likely. This equation implies a trade-off between the peak pressure magnitude and pulse duration, with increasing impact velocity increasing pressure while also reducing duration. Table 2 shows the flyer thickness, impact velocity, impact shock energy, and result for a few of initial calculations. The critical energy, $E_c$, for the N-110 model appeared to be between 3.1 and 3.8 MJ/m$^2$ for our metallic flyers. This value provided a criterion for judging the launcher design as it evolved. Note that this critical energy is specific to the model in the context of our analysis, and should not be taken as a critical energy value for actual N-110 HE.

Table 2: Sample of 1 cm diameter flyer impacts and SDT response of PBXN-110 IGRB model in CTH

| Flyer Material | Thickness (cm) | Velocity (km/s) | Pulse Duration, τ (μs) | Pulse depth (cm) | Pulse Pressure, P (GPa) | Energy, E (MJ/m$^2$) | SDT | Run distance (cm) |
|---|---|---|---|---|---|---|---|---|
| **Steel** | 0.12 | 1.5 | 0.36 | 0.14 | 8.4 | 3.8 | Yes | 0.9 |
| **Steel** | 0.25 | 1.5 | 0.75 | 0.30 | 8.4 | 8.0 | Yes | 0.6 |
| **Ti6V4Al** | 0.12 | 1.5 | 0.35 | 0.13 | 7.6 | 3.1 | No | -- |
| **Ti6V4Al** | 0.12 | 1.75 | 0.33 | 0.14 | 9.3 | 4.2 | Yes | 0.7 |
| **Ti6V4Al** | 0.25 | 1.75 | 0.70 | 0.28 | 9.3 | 8.9 | Yes | 0.4 |

Results of preliminary calculations indicated that longer run distance was required for thinner flyers, which produce thinner, shorter duration, peak pressure pulses. This is illustrated in Fig. 2. But these thin-pulses were calculated to produce SDT when the depth of the peak pressure pulse was significantly less than the 0.3 cm minimum indicated by wedge test data. Walker [11] pointed out the possibility for initiation even after the peak shock pressure had been relieved. So it would be possible to propel a thinner, lighter flyer to higher velocities and achieve detonation. At these higher velocities the higher shock pressure compensates for the shorter pulse duration in achieving $E_c$. However, we did find 0.1 cm thickness to be a lower limit for flyer thickness for velocities up to 2.2 km/s, and this is attributable to the reduction in pulse duration.

Having established a shock energy threshold for producing SDT, launcher design 3-D CTH simulations were carried out. Our initial designs for propelling the flyer with a detonation wave involved a small polymer buffer having the same diameter as the flyer and similar thickness, as illustrated in Fig. 1. These simulations used a cell size of 0.020 cm. The HE driving the buffer/flyer was with N-110 IGRB and JWL. This was initiated by a programmed burn of LX-14 having the same mass and size as the booster planned for use in testing. The flyers and buffers EOS were modeled using tabular equations of state. The Steinberg-Guinan-Lund viscoplastic model (Steinberg [12]) was used for flyer material strength. The buffer materials examined were polycarbonate, acrylic, and polystyrene. Flyer materials included 4340 steel, Ti6V4Al, tungsten heavy alloy, and 304 stainless steel.

These configurations consistently resulted in flyer spall and break up. Velocities for the spall fragment exceeded 2.0 km/s, but lacked sufficient mass to create SDT in the target. Buffer thickness and diameter were increased in an attempt to reduce spall stresses in the flyers. However, the thicker barrier reduced flyer velocities below acceptable levels. But overall Ti6V4Al seemed to be the most resistant to spall and achieved the highest velocities, so it was used in the rest of the design study.

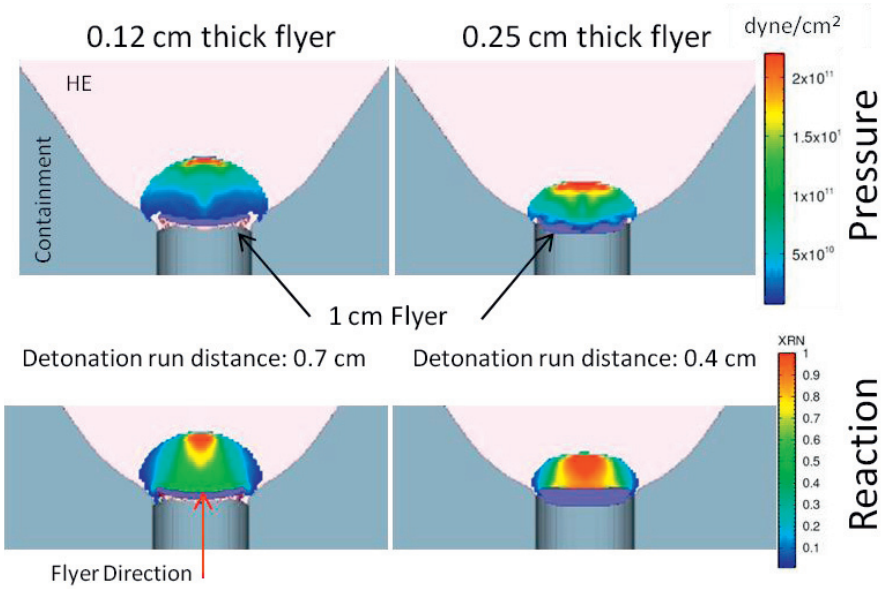


Fig. 2. Thick and thin Ti6V4Al flyer impact and resulting detonation reaction. Impact velocity is 1.75 km/s.

One critical realization made during this initial study was that a larger steel bezel around the flyer reduced breakup. The bezel seemed to produce two somewhat similar effects. One, the bezel increased the apparent diameter of the flyer to equal that of the explosive. This allowed a more planar shock to impinge on the flyer, reducing the acceleration gradient across the flyer. This wave was a combination of shock from the buffer and shock transmitted through the bezel, both driven by the launcher HE detonation wave. Two, the bezel reduced relief wave pressures by acting as an acceptor for any radial components of shock in the flyer. In practical terms this meant the flyer and bezel would need to be constructed with an interference fit, but this was not difficult to implement.

Buffers attempted up to this point had a thickness of near that of the flyer, with diameters the same as the flyer or the flyer-bezel assembly. Alternatively we considered a buffer that extended into the HE directly behind the flyer. The result was a significant reduction in shock transmission that caused breakup of the flyer. The mature shock front that formed in the longer buffer appeared to impart a less abrupt shock to the flyer, but total momentum transmission was still enough to propel the flyer above 2.0 km/s. The longer buffer also created compressed stream of buffer material that would impede reaction product flow through the bezel. Fig. 3 illustrates our initial attempts on this approach. Resolution for this calculation was 0.025 cm. This design achieved flyer velocity of 2.5 km/s. Minor flyer spall did occur, but was greatly reduced compared to prior designs.

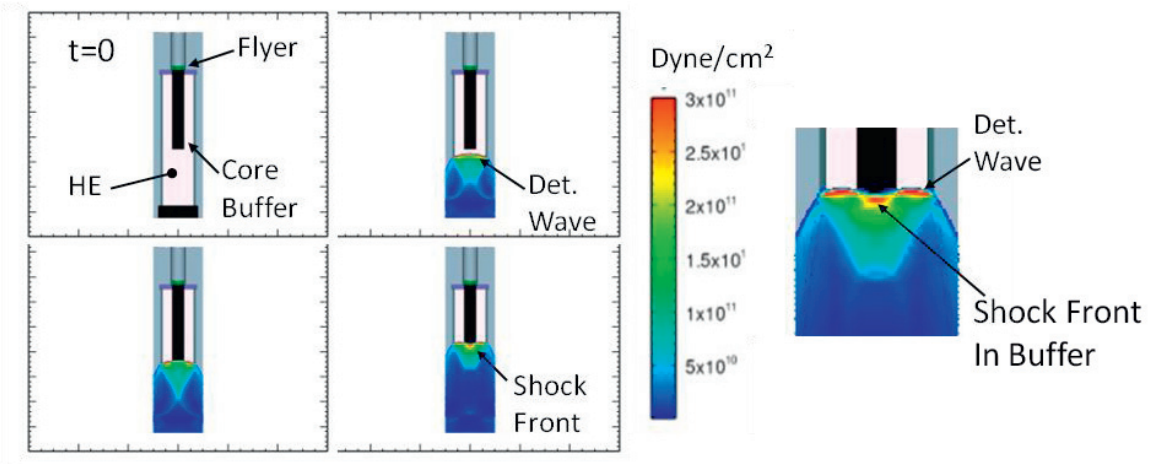


Fig. 3. Initial design of HE compressed core buffer

The compressed core buffer design was further refined with simulations. Geometry changes were made to the bezel that further reduced reflected stress waves in the flyer. This completely eliminated flyer spall and fracture. Additionally, the buffer shape was changed from a column to a cone to maximize the HE content of the launcher.

Flyer diameter was reduced to approximately 0.6 cm diameter, having a thickness of 0.15 cm. This was determined by incrementally reducing the flyer diameter until SDT failure. These were simplified simulations with 0.15 cm thick Ti6V4Al flyer given an initial velocity of 2.5 km/s. This configuration was calculated to produce a peak pressure pulse in excess of 20 GPa, and deposit shock energy, $E$, of approximately 8.5 MJ/m$^2$. This is well above the threshold of 3.8 MJ/m$^2$ determined in initial calculations. Resolution for these calculations was 0.020 cm.

The lower bound for the diameter of a 0.15 cm thick was found to be approximately 0.5 cm. This corresponded reasonably with the reported experimental failure diameter. Achieving SDT was also reasonable considering that the diameter of the target HE where the impact occurs is greater than 1 cm. The high shock pressures, greater that 20 GPa, expanded to fill this region. This pressure was well above maximum wedge test pressures.

All simulations up to this point had used N-110 as both the launcher driver and target. Practical considerations of fabrication cost pushed us toward C-4 as the driver HE. Simulations indicated that C-4 produced slightly a lower velocity, but SDT in the target was still achieved. The C-4 was modelled with the HVRB model and a tabulated EOS. The slight difference in velocities is likely due to the higher accuracy of the C-4 EOS. Fig. 4 shows the velocity profile for both N-110 and C-4 drivers and flyer launch with a C-4 driver. The early time velocity variation in the flyer as seen in the contour plots in Fig. 4 are due to launch pulse wave reflections.

The velocity plot in Fig. 4 also illustrates that the flyer achieves maximum velocity within about 3 μs of the arrival of the shock from the buffer. There is very little acceleration after that time. This indicates that the primary propulsive mechanism is momentum transfer from the shock wave. Pressures from expanding buffer appeared to contribute very little as the flyer moves toward the target. This rapid acceleration is critical to the design since the target HE is intended to be only a few centimetres away. In contrast, Meier [1] and Marsh [2] described the FST flyer as being accelerated by momentum transfer and their expanding buffer. This may partially explain the higher flyer velocities obtained with the FST.

Impact and resulting SDT are illustrated by calculation results shown in Fig. 5. The arrangement is similar to the final design, having a C-4 driven Ti6V4Al flyer and a long cone-shaped buffer. Note that fully reacted target HE at this point in the calculation is not necessarily indicative of a self-sustaining detonation, only that the reaction rate criteria had been satisfied. However, SDT did result in the simulation shown. The expanding buffer material is seen to be contacting the target HE simultaneously with the flyer. Calculations without the flyer, and without the buffer, indicated that the buffer neither significantly impeded nor aided the flyer in producing SDT.

At this point in the study we had fixed the design of the launcher and part fabrication was started. The design used a solid polystyrene buffer to ensure easy fabrication and reduce the possibility of breakage during assembly and handling. By contrast, the FST used a porous polystyrene buffer. Also, the FST buffer extended the full length of the explosive driver, while our buffer extends in about half way. The FST work considered a number of different foam buffers. These porous materials appear to be critical in propelling intact flyers to velocities greater than 3 km/s.

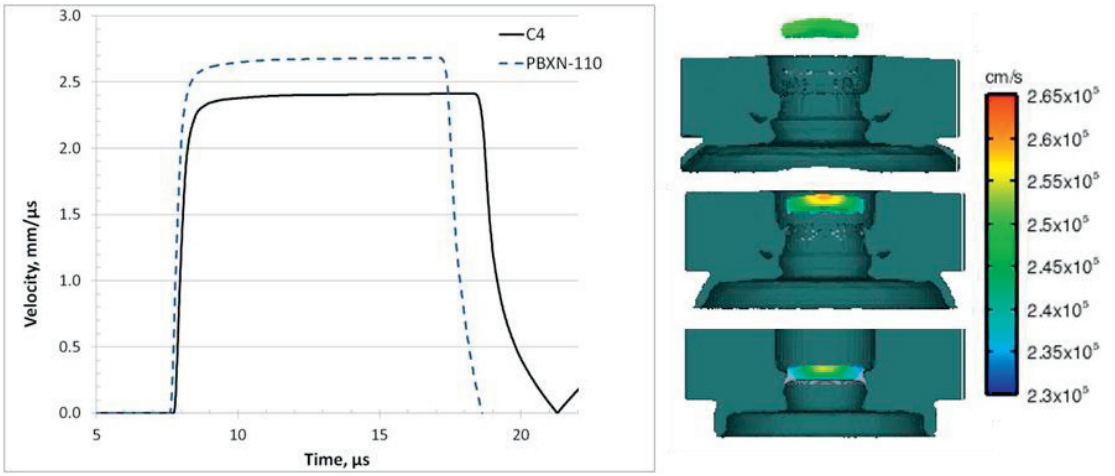


Fig. 4. Flyer launch velocity, buffer and reaction products are not shown in the images on the right

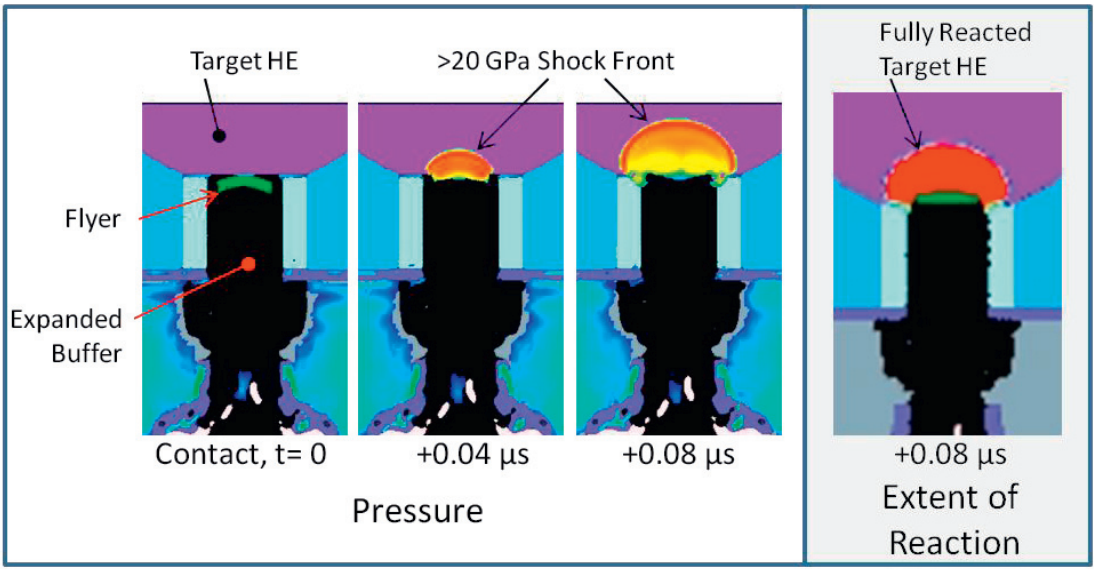


Fig. 5. Flyer impact and resulting SDT, impact shock on left, extent of reaction ignition and growth on right

The FST used buffer densities as low as 0.27 g/cc. To find out if our design would produce higher velocities with a porous buffer we substituted 0.76 g/cc porous polystyrene for our 1.0 g/cc polystyrene buffer. Our choice of 0.76 g/cc was based primarily on keeping the material as polystyrene and the availability of a reliable EOS. These follow-on simulations used a tabular EOS of the same origin as the 1.0 g/cc buffer. A simulation cell size of 0.020 cm was used.

The porous buffer produced a higher flyer velocity of 3.1 km/s. Fig. 6 compares buffer shock pressures and resulting impulse for the 1.0 g/cc and 0.76 g/cc buffers. These results were from a point at the center of the buffer and 0.06 cm from the buffer/flyer boundary. Impulse from the porous buffer is calculated to be 13% higher than the solid buffer. As the plot shows, the impulse advantage of the porous buffer does not happen by the time the shock pressure peaks, but is due to slower fall off. The pressure peak in the porous buffer is higher as a result of the stronger reflection that occurs at the flyer/buffer surface. This is attributable to the lower shock impedance of the porous buffer compared to the solid buffer, even in the highly compressed state. As expected, the porous buffer produces lower peak pressure in the flyer, 38.5 GPa, compared to 42 GPa for the solid buffer. Clearly, higher velocities and lower pressures in the flyer would have been advantageous in our design. However this realization came too late for changes to the test items.

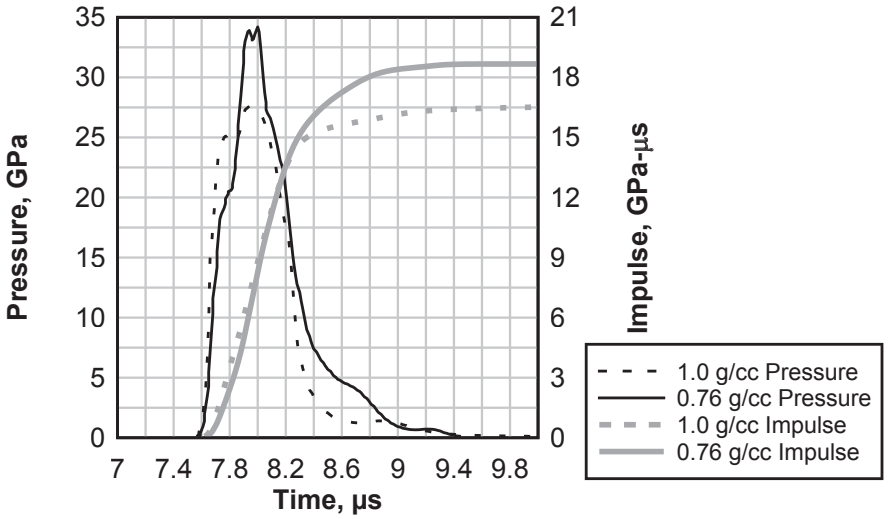


Fig. 6. Comparison of propulsive pressures in buffer, near buffer/flyer interface, for solid (1.0 g/cc) and porous (0.76 g/cc) buffers

## 5. Testing

Three tests were done with the launcher in a stand-alone configuration, and several were conducted with the launcher integrated into a full system prototype containing a target HE. Only the three stand-alone tests will be discussed in detail, and the prototype results will be briefly summarized.

Tests 1 and 2 were done with the core subassembly only, having no containment beyond the steel bezel. In Test 3 a polycarbonate tube was added to the open end of the bezel to provide containment of propulsive gasses that might accelerate the flyer. A major difference between the test setup and the design goal was the flight distance of the flyer. The design requirement was that the flyer travel about 2.2 cm, while in the stand-alone tests it traveled tens of centimeters. C-4 was used in the launcher for all three tests.

Fig. 7 shows the setup for the stand-alone tests. The flyer was launched and then impacted a breakscreen and soft-catch recovery bundle. Flight timing was provided by a breakwire on the launcher and the breakscreen. The breakwire was on the launcher OD, just aft of the bezel. The launcher was mounted in a steel plate intended to shield the flyer and soft-catch from expanding launcher debris. The distance between the mounting plate and the breakscreen was 50 cm, 25 cm, and 15 cm for tests 1, 2, and 3 respectively. Celotex was used for the soft-catch material.

A Photronics SA5 camera was used to capture video of the flyer traveling between the launcher and breakscreen. Camera frame rate was 125K in tests 1 and 2, and 160K in test 3. In early time the flyer was completely obscured due to camera overexposure caused by bright, hot gases emerging from the launcher muzzle. Mid-flight the flyer was captured in 8, 6, and 3 frames for tests 1, 2, and 3 respectively.

Flyer velocities measured by breakscreen timing and video are listed in Table 3. These velocities compared well with the 2.4 km/s velocity result from the simulation using C-4 as a driver. There were various uncertainties in the tests measurements and that analysis of these is beyond the scope of this paper. However, the general agreement between the two different methods and test-to-test does lend confidence in the data.

Table 3: Flyer velocity data (Beus, 2011[13])

| | High Speed Video | | Breakscreen | |
|---|---|---|---|---|
| Test | Frame rate | Avg. Velocity (m/s) | Distance (m) | Avg. Velocity (m/s) |
| 1 | 125K | 2380 | 0.5 | 2150 |
| 2 | 125K | 2380 | 0.25 | 2450 |
| 3 | 160K | 2410 | 0.15 | Failure |

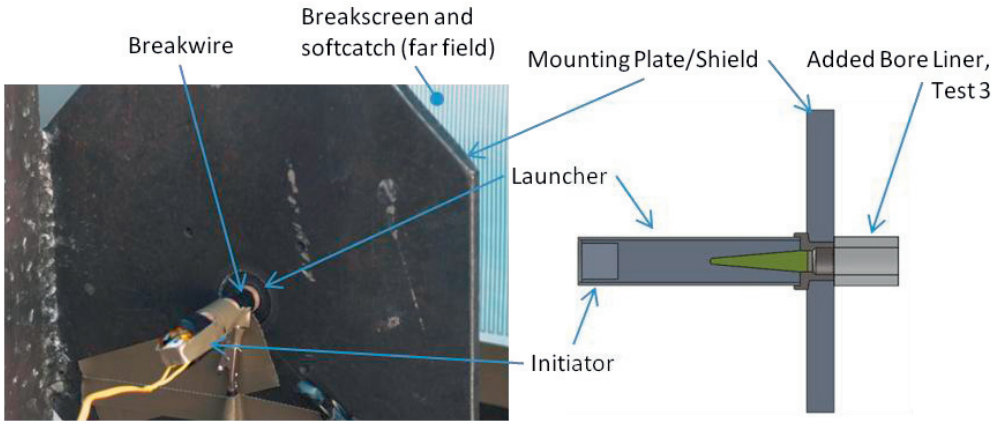


Fig. 7. Launcher testing setup

Ideally the flyer was to launch intact and maintain a planar orientation in flight. Perforations of the breakscreens and soft-catch served as a witness to the orientation of the flyer at impact. In all three tests very clean holes approximately the diameter of the flyer resulted in breakscreens.

Fig. 8 shows an unfired flyer placed in the breakscreen perforation created in test 1. It was possible that each flyer happened to be in the correct orientation on impact to create a planer profile hole, but this seemed improbable for three tests since each was at different distances. After testing, calculations using Corvid's in-house six degree-of-freedom aerodynamics model indicated the flyer would be stable to distances greater than 50 cm. Additional CTH calculations, which included air, indicated the flyer would be stable out to at least 5 cm. 5 cm was the reasonable run time limit for the simulation.

All three flyers were recovered from the soft-catch intact, confirming launch without breakup. Two flyers had minor indications of spall.

Fig. 9 shows the three recovered flyers, and a pristine flyer (P). Spall appears to have occurred on the center of the impact face of flyers from test 1 and 2. The spall presents as a fairly neat round pit. Tooling marks were noticeable in the center of pristine flyers. It is possible that cold working or small fractures were caused by turning forces, and these defects acted as antecedents to the spall. All flyers had mass loss of less than 12%. The test 3 flyer suffered the most erosion and a slight increase in diameter. This might be attributable to the addition of the polycarbonate tube to the launcher muzzle causing increased ablation by expanding buffer material and HE reaction products.

Having success in the launcher stand-alone tests, testing was done with launcher integrated into a prototype system where the goal was initiate target HE in the system with the flyer. In 4 of 5 system tests the target high explosive was detonated by projection of the flyer from the launcher. Details of these tests are beyond the context of this paper. However, the results were found satisfactory and have motivated further development of the launcher.


Fig. 8. Breakscreen Perforation.

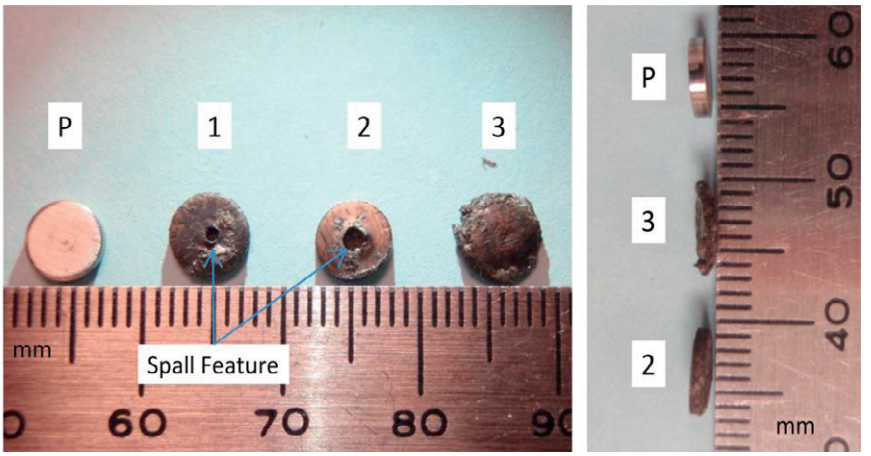


Fig. 9. Recovered Flyers. Impact surface shown on left, edge on right.

## 6. Conclusions

Computer simulations were successfully used to develop and refine a unique small-scale high-velocity launcher. Simulations allowed for the mechanics of launch to be studied, as well as the intended effects on a reactive target. This approach enabled the launcher to go from concept to a robust working prototype in less than nine months, and was accomplished within the context of a much more complex system design effort.

Flyers approximately 0.6 cm in diameter had a predicted launch velocity of 2.4 km/s. Measured velocities were within -10.4% to +0.4% of the predicted value. Simulations were used to develop buffers and containment that eliminated issues of flyer breakup. Testing showed that the flyers were launched intact, confirming simulation predictions. Stable 2 cm flight was predicted by design calculations, and test results indicated stable flight over a distance of up to 50 cm. Overall simulation results agreed well with test data.

Subsequent simulations indicate performance improvement with porous buffers, with velocities above 3 km/s clearly obtainable. This and other design refinements will be incorporated into future versions. This work demonstrates the value of hydrocode modeling in the design of devices where shock mechanics are primary to function. Application of this launcher concept, and the approach used to develop it, extend beyond use in a munition. Other applications might include materials characterization at high strain rates, EOS work, and disposal of unexploded ordnance.

## Acknowledgements

We would like to thank Donald Littrell of the US Air Force Research Lab, RWMW, for his support of this work.

## References

[1] MIL-STD-1316E, *Department of Defense Design Criteria Standard: Fuse Design, Safety Criteri for,* 10 July 1998, Distribution Statement A. Approved for public release

[2] Meier, J. (1992). Problems Associated with Launching Hypervelocity Projectiles from the Fast Shock Tube. *Hypervelocity Impact Symposium*. Los Alamos, New Mexico: Los Alamos National Labortories.

[3] Marsh, S. (1991). Hypervelocity Plate Acceleration. *APS Conference on Shock Compression of Condensed Matter.* Williamsburg Virgina: Los Alamos National Laboratory.

[4] G. T. Sutherland, E. R. (1993). Shock wave and detonation wave response of selected HMX based research explosives with HTPB binder systems. AIP Conference Proceedings, High-pressure science and technology (pp. 1413-1416). Colorado Springs, Colorado: AIP.

[5] OConnor, E. J. (2001). Validation Of Reactive Models For PBXN-110. 19th JANNAF Propulsion Systems Hazards Subcommittee Meeting (pp. 245-249). Monterey, California: NAVAL SURFACE WARFARE CENTER DAHLGREN DIV VA.

[6] Cooper, P. (1997). *Explosives Engineering.* New York: Wiley-VCH.

[7] Hull, L. M. (2002). Impact Initiation Of PBXN-110 And PBX-9501. *30th Explosives Safety Seminar* (p. 27). Atlanta, Georgia: Los Alamos National Laboratory.

[8] Sandia Corporation. (2012, 04 11). *CTH Shock Physics*. Retrieved 5 01, 2012, from Sandia National Labratories: http://www.sandia.gov/CTH/index.html

[9] P. J. Miller, G. T. (1995). Reaction rate modeling of PBXN-110. *Proceedings of the conference of the American Physical Society topical group on shock compression of condensed matter* (pp. 413-416). Seattle, Washington: AIP Conf. Proc. 370.

[10] James, H, (1988) Critical energy criterion for the shock initiation of explosives by projectile impact. *Propellants, Explosives, Pyrotechnics*, Vol. 13, Issue 2, Pages 35-41

[11] Walker, F., Wasley, R. (1976), A General Model for the Shock Initiation of Explosives, *Propellants, Explosives, Pyrotechnics*, Vol. 1, Issue 4, Pages 73-80

[12] Steinberg, D. (1996). Equation of State and Strength Properties of Selected Materials. Livermore California: Lawrence Livermore National Laboratory.

[13] Beus, R. (2011, December 21). Personal Communication. Mesa Arizona: Nammo-Tally.